

Atomistic Simulation of Defect Properties in BCC Tantalum

L.H. Yang, P. Soderlind, J.A. Moriarty

This article was submitted to
10th International Ceramics & 3rd Forum on New Materials, Florence,
Italy, July 14-18, 2002

April 23, 2002

U.S. Department of Energy

Lawrence
Livermore
National
Laboratory

DISCLAIMER

This document was prepared as an account of work sponsored by an agency of the United States Government. Neither the United States Government nor the University of California nor any of their employees, makes any warranty, express or implied, or assumes any legal liability or responsibility for the accuracy, completeness, or usefulness of any information, apparatus, product, or process disclosed, or represents that its use would not infringe privately owned rights. Reference herein to any specific commercial product, process, or service by trade name, trademark, manufacturer, or otherwise, does not necessarily constitute or imply its endorsement, recommendation, or favoring by the United States Government or the University of California. The views and opinions of authors expressed herein do not necessarily state or reflect those of the United States Government or the University of California, and shall not be used for advertising or product endorsement purposes.

This is a preprint of a paper intended for publication in a journal or proceedings. Since changes may be made before publication, this preprint is made available with the understanding that it will not be cited or reproduced without the permission of the author.

This report has been reproduced directly from the best available copy.

Available electronically at <http://www.doe.gov/bridge>

Available for a processing fee to U.S. Department of Energy
and its contractors in paper from
U.S. Department of Energy
Office of Scientific and Technical Information
P.O. Box 62
Oak Ridge, TN 37831-0062
Telephone: (865) 576-8401
Facsimile: (865) 576-5728
E-mail: reports@adonis.osti.gov

Available for the sale to the public from
U.S. Department of Commerce
National Technical Information Service
5285 Port Royal Road
Springfield, VA 22161
Telephone: (800) 553-6847
Facsimile: (703) 605-6900
E-mail: orders@ntis.fedworld.gov
Online ordering: <http://www.ntis.gov/ordering.htm>

OR

Lawrence Livermore National Laboratory
Technical Information Department's Digital Library
<http://www.llnl.gov/tid/Library.html>

ATOMISTIC SIMULATION OF DEFECT PROPERTIES IN BCC TANTALUM

Lin H. YANG, Per SÖDERLIND, and John A. MORIARTY

Lawrence Livermore National Laboratory, Livermore, California 94551, USA

The fundamental atomic-level properties of point and line defects in bcc Ta have been simulated by means of quantum-based multi-ion interatomic potentials derived from the model generalized pseudopotential theory (MGPT). The potentials have been applied to the calculations of point defect formation and migration energies. The results are then compared with the *ab-initio* electronic-structure results and experimental data, which in turn provide rigorous validation tests of the MGPT potentials. Robust and accurate two- and three-dimensional Green's function (GF) techniques have been developed for static and dynamic simulations of single $a/2\langle 111 \rangle$ screw dislocation properties in bcc Ta. The transformation of the dislocation core under the influence of external stress was studied in detail using static GF method. Finite-temperature GF simulation reveals multiple-kink (thermal-kink) formation under an applied stress and the corresponding thermal-kink configuration entropy is estimated to be around $5.23k_B$.

1. INTRODUCTION

In the development of modern materials theory there is a growing awareness of the importance of a fundamental understanding of the role of special lattice defects. For example, most physical properties of crystalline materials are affected more or less by the presence of dislocations and point defects and the interactions between them. In many cases these are dominated by the elastic strain field which, for distances more than a few atomic spacing from the center of the dislocation, is described well by linear continuum elasticity. However, it has been demonstrated¹ that the continuum description, which excludes the short-range details of important non-linear effects, cannot account for the intrinsic dislocation-lattice coupling which is the source of the anisotropic crystal plasticity in bcc metals. Therefore, a detailed description of the dislocation properties at atomic scale with proper boundary conditions has become increasingly important to advance the modern dislocation theory in crystal plasticity. The other important problem in atomistic-simulation studies of dislocations and other lattice defects is how to calculate the interaction potentials describing interatomic forces with sufficient accuracy. Specifically, it has been shown that the multi-ion *d*-state

interactions play an important role for bcc transition metals with partially filled d -bands, and therefore any proposed interaction scheme must explicitly contain angular-force contributions². In this paper, we present our simulation results of fundamental atomic-level properties of point and line defects in bcc Ta using quantum-based multi-ion interatomic potentials derived from the model generalized pseudopotential theory (MGPT). Some validation tests of the MGPT potentials are presented in comparing point defect formation and migration energies with the *ab-initio* electronic-structure results and the experimental data. Robust 2D and 3D GF techniques have been used to simulate static and dynamic dislocation properties. In particular, the $a/2\langle 111 \rangle$ dislocation core properties under the influence of applied shear loading and temperatures were extensively studied using the MGPT-GF technique.

2. COMPUTATIONAL METHODS

2.1. *Ab-initio* electronic structures methods

For the point defect calculations, we used both full-potential linear muffin-tin orbital³ (FP-LMTO) and plane-wave pseudopotential⁴ (PP) techniques. Both methods are fully implemented within first-principles density functional theory (DFT). Because the PP method can handle larger number of atoms and perform structural relaxation in a much faster fashion, it is used to obtain relaxed defect structures as input into the FP-LMTO calculations. Such a combination of using two *ab-initio* techniques offers a very efficient and accurate approach for calculating defect structures and energetics.

2.2. MGPT interatomic potentials

The present calculations in Ta have been carried out using quantum-based, multi-ion interatomic potentials derived from model generalized pseudopotential theory (MGPT)². This approach is based on the corresponding first-principles generalized pseudopotential theory (GPT)⁵, which provides a rigorous real-space expansion of the total energy for a bulk transition metal in the form

$$E_{tot}(\mathbf{R}_1 \dots \mathbf{R}_N) = NE_{vol}(\Omega) + \frac{1}{2} \sum'_{i,j} v_2(ij; \Omega) + \frac{1}{6} \sum'_{i,j,k} v_3(ijk; \Omega) + \frac{1}{24} \sum'_{i,j,k,l} v_4(ijkl; \Omega) \quad (1)$$

, where $\mathbf{R}_1 \dots \mathbf{R}_N$ denote the positions on the N ions in the metal, Ω is the atomic volume, and the prime on each sum over ion positions excludes all self-interaction terms where two indices are equal. The leading volume term in this expansion, E_{vol} , as well as the two-, three-, and four-ion interatomic potentials, v_2 , v_3 , and v_4 , are volume

dependent, but structure independent quantities and thus transferable to all bulk ion configurations. The angular-force, multi-ion potentials v_3 and v_4 reflect contributions from partially-filled d -bands and are generally important for central transition metals. Within the MGPT framework⁵, these potentials are systematically approximated by introducing canonical d bands and other simplifications to achieve short-ranged, analytic forms, which can then be applied to both static and dynamic simulations with the Green's function techniques described below. To compensate for the approximations introduced into the MGPT, a limited amount of parameterization is allowed in which the coefficients of the modeled-potential contributions are constrained by experimental or volume-dependent *ab-initio* theoretical data. The details of this parameterization for Ta, together with extensive validation tests of the potentials, are discussed in Ref. 1.

2.3. MGPT Green's function simulation method

For the study of dislocation properties, a method for dynamically updating the boundary conditions of atomistic simulations⁶ has been used. The boundary conditions for 2D and 3D defect cells are evaluated using line⁷ and point⁸ force distributions, respectively. In this static and dynamic flexible boundary condition method, the simulation box is divided into three regions: atomistic, GF, and continuum. In the continuum region, the atomistic positions are initially determined according to the anisotropic elastic displacement field⁷ for a dislocation line defect at the center of the atomistic region. Complete atomistic relaxation or updating is performed in the atomistic region according to the interatomic forces generated from Eq. (1). Forces develop in the GF region as relaxation or propagation is achieved in the atomistic region are then used to relax or propagate atoms in all three regions by the 2D or 3D lattice and elastic GF solutions for line⁷ or point⁸ forces.

3. DEFECT AND MECHANICAL PROPERTIES OF BCC TA

3.1. Vacancies and self-interstitials

Point defects, including vacancies, self-interstitials and impurities, can have an important impact on the mechanical properties of metals. In the calculations of vacancy and interstitial formation energies, we calculated the relaxed total energy $[E_{\text{tot}}(N, \Omega_N)]$ for a supercell with N atoms in a volume Ω_N and with periodic boundary conditions applied in all three directions. At zero pressure, the formation energy for the defect is defined

as $E^f = E_{\text{tot}}(N, \Omega_N) - NE(\Omega_0)$, where $E(\Omega_0)$ is the energy per atom of the bulk solid at the equilibrium atomic volume Ω_0 .

Table I summarizes calculated vacancy and self-interstitial formation and migration energies and formation volumes for Ta using FP-LMTO, PP, and MGPT methods, together with available experimental data⁹. For the self-interstitial formation energy, only the <110> split-dumbbell configuration is presented here, which is found to be the lowest-energy configuration compared to other self-interstitial defects. The same conclusion is also found in bcc Mo¹⁰. The migration energy for the point defects is determined from $E^m = E^{\text{saddle}} - E^f$, where E^{saddle} is the formation energy of the defect at the saddle point. The optimized migration paths are found to be along <111> for both the vacancy and self-interstitials, with the latter corresponding to the so-called jump and rotation path. Overall, there is good agreement between theory and experiment and between the electronic-structure results and the MGPT results.

TABLE 1

Vacancy and <110> split-dumbbell self-interstitial formation energies E_{vac}^f and E_{int}^f , migration energies E_{vac}^m and E_{int}^m , and formation volumes Ω_{vac}^f and Ω_{int}^f for bcc Ta. The MGPT vacancy and self-interstitial results were obtained from 250-atom and 1800-atom supercell calculations, respectively. The PP and FP LMTO vacancy results were obtained from fully relaxed 54-atom supercell calculations, using ten special k-points, except the FP LMTO vacancy migration energy where a 36-atom supercell was used. The PP self-interstitial results were obtained from corresponding 128-atom supercell calculations, which are slightly different from 48-atom supercell calculations reported in Ref. 1. Migration energies were calculated along <111> migration paths, as described in the text. The experimental data is from Ref. 9.

	$E_{\text{vac}}^f(\text{eV})$	$E_{\text{vac}}^m(\text{eV})$	$\Omega_{\text{vac}}^f/\Omega_0$	$E_{\text{int}}^f(\text{eV})$	$E_{\text{int}}^m(\text{eV})$	$\Omega_{\text{int}}^f/\Omega_0$
MGPT	2.89	0.78	0.53	6.30	0.50	0.40
PP	3.10	0.90	0.60	6.43	0.55	0.31
FP LMTO	3.10	0.74				
Experiment	2.8-3.1	0.7				

3.3. $a/2\langle 111 \rangle$ screw dislocation properties

The low-temperature and high-strain-rate plasticity of bcc metals is controlled by the intrinsic core properties of $a/2\langle 111 \rangle$ screw dislocations. Unlike the highly mobile edge dislocations in these metals, the motion of the screw dislocation is severely restricted by the nonplanar atomic structure of its core, resulting in low mobility and high Peierls stress. However, under the influence of external loading and temperature, the core

structure undergoes a transformation in the process of dislocation motion. In this section, we present our static and dynamic simulations of individual $a/2\langle 111 \rangle$ screw dislocations in bcc Ta using MGPT-GF technique.

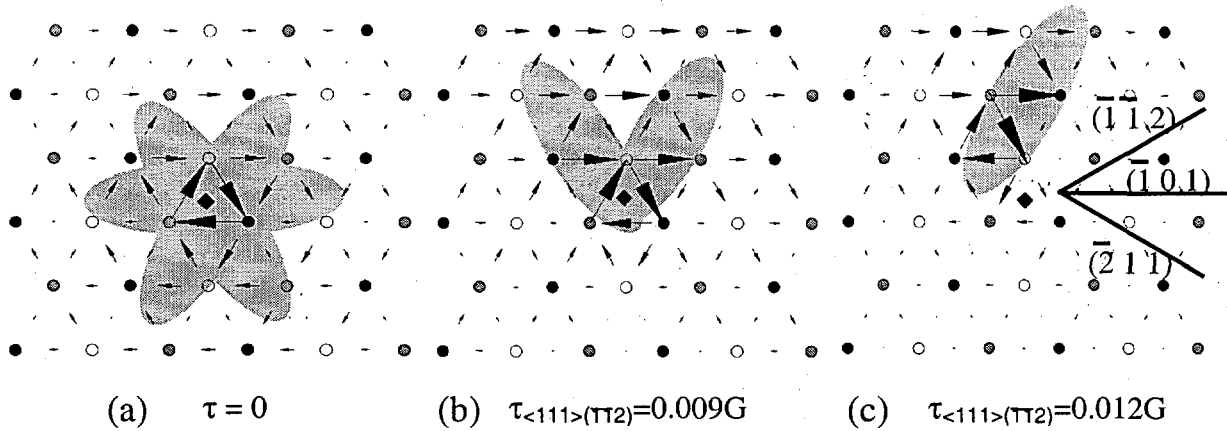


FIGURE 1

The screw-component displacement maps of the dislocation core in Ta under applied pure shear stress in the $\langle 111 \rangle$ direction on the $(-1 -1 2)$ plane. The $\langle 111 \rangle$ screw component of the relative displacement of neighboring atoms due to the dislocation is represented by an arrow between the two atoms. The symmetry of the core configuration is decreasing with increasing stress. The applied stress is in units of shear modulus in the $\langle 111 \rangle$ direction, i.e. $G = 0.625\text{Mbar}$ for Ta. The calculated Peierls stress is $0.0102G$. The stress-free elastic center associated with the screw dislocation is indicated by a diamond symbol.

3.3.1. Stress-free ground-state core configuration

The stable ground-state core configuration of the $a/2\langle 111 \rangle$ screw dislocation is centered among three $\langle 111 \rangle$ atomic rows forming a triangular prism. Around these three rows the near-neighbor atoms are positioned on a helix that winds up in a clockwise or counter-clockwise manner, depending on the location of the elastic center and the sign of the Burgers vector \mathbf{b} . In the present work, the atomic core structure in bcc Ta has been simulated using a 2D MGPT-GF technique in cylindrical geometry, with periodic boundary conditions along the $\langle 111 \rangle$ direction. Our results reveal that a nearly isotropic but still three-fold symmetric and doubly degenerate core, whose detailed structure is easily displayed using the differential displacement method¹¹. The calculated screw-component map for Ta is shown in figure 1a. The MGPT dislocation core structure is comparable with the results obtained by other authors using different

potentials and using electronic-structure techniques¹², where their reported dislocation core structures show completely isotropic core configuration.

3.3.2. Core configurations under applied stress

When the straight dislocation is under external loading, the applied stress exerts the Peach-Koehler force on the $a/2\langle 111 \rangle$ screw dislocation. If the applied stress is large enough to overcome the Peierls barrier, the straight dislocation starts to move on the maximum resolved shear stress plane. During the course of loading with increasing stress, the dislocation core undergoes a transformation due to symmetry breaking induced by the external forces. In the present work, we only consider external loading corresponding to the application of a pure shear stress (τ) parallel to the Burgers vector and resolved on the $(-1 -1 2)$ plane.

The effects of the applied stress on the dislocation core are shown in figures 1b and 1c. For stress levels somewhat lower than the corresponding critical resolved shear stress (τ_P), the core extends and spreads into $(-1 1 0)$ and $(0 -1 1)$ planes, resulting in a reduction of symmetry from nearly six-fold to two-fold. As the applied stress is increased slightly higher than τ_P , the dislocation starts to move by extending its core along the $(0 -1 1)$ plane and constricting the other part of the core that is spread along the $(-1 1 0)$ plane. This type of core transformation eventually reduces the corresponding core symmetry from two-fold to one-fold. The dislocation actually moves in a zigzag pattern on successive $\{110\}$ planes, so the effective slip plane is in fact a $\{112\}$ plane for bcc Ta.

3.3.3. Multiple-kink formation at finite temperatures

At finite temperatures, the straight dislocation is under the influence of thermal fluctuations and thus the possibility of forming double kinks is increased¹³. In the present work, we have considered finite-temperature GF simulation of dislocation motion under pure shear loading at a level about 10% below the calculated Peierls stress ($\tau_P = 0.0102G$). The simulation cell is constructed in a cylindrical geometry with periodic boundary conditions along the dislocation line direction. The atomistic region contains a radius of $40b$ ($b=2.86\text{\AA}$ is the length of the Burgers vector) and $200b$ in length. The simulation was performed at 300K.

Our simulation results reveal multiple-kink formation along the screw dislocation line. A snapshot of the atomistic kink structure is displayed in figure 2b. It is also possible to estimate the configuration entropy of forming thermal kinks by counting all possible double-kink configurations under various loading conditions. Statistically averaging over

35 loading conditions gives an average kink width of $3.7b$ and an estimate of the configuration entropy of about $5.23k_B$.

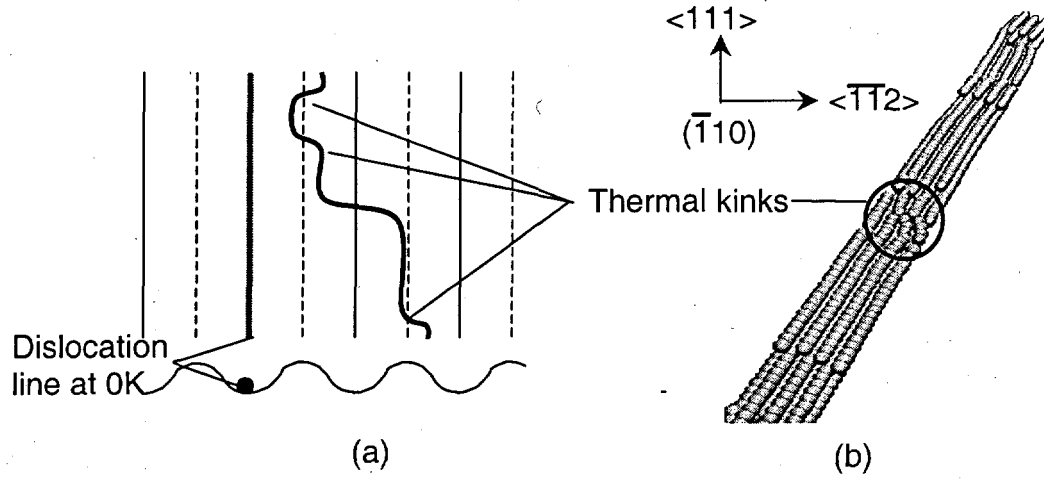


FIGURE 2

(a) Schematic drawing of thermal-kink formation at finite temperatures. (b) A snapshot of thermal-kink formation along the $\langle -1 -1 2 \rangle$ direction on the $(-1 1 0)$ plane.

4. DISCUSSION

In this paper, we have presented our work on quantum-based atomistic simulation of materials properties in bcc Ta. Central to this work is the development, from fundamental quantum mechanics, of robust many-body interatomic potentials for bcc transition metals via model generalized pseudopotential theory (MGPT), providing close linkage between *ab-initio* electronic structure calculations and large-scale static and dynamic atomistic simulations. Successful application and validation of MGPT potentials were demonstrated by comparing point defect formation and migration energies with the *ab-initio* electronic-structure results and experimental data. Robust 2D and 3D GF techniques have been used to simulate static and dynamic screw dislocation properties. Under external loading, our static simulation reveals a symmetry reduction in the dislocation core structure during the process of dislocation motion. At finite temperatures, the thermal fluctuations induce multiple-kink formation along $\{110\}$ planes in our dynamic GF simulations. The configuration entropy associated with the thermal-kink formation is estimated to be around $5.23k_B$.

ACKNOWLEDGMENTS

This work was performed under the auspices of the U.S. Department of Energy by the University of California Lawrence Livermore National Laboratory under contract number W-7405-ENG-48. This work was also supported in part by a grant of computer time from the US Department of Defense High Performance Computing Modernization Program, at the Aeronautical Systems Center-Major Shared Resource Center, on the IBM-SP2 and IBM-SP3.

REFERENCES

- 1) L.H. Yang, P. Söderlind and J.A. Moriarty, *Phil. Mag. A* **81** (2001) 1355; and references therein.
- 2) J. A. Moriarty, *Phys. Rev. B* **38** (1988) 3199.
- 3) J. M. Wills, unpublished (2000).
- 4) L.H. Yang, *Industrial Strength Parallel Computing* (Morgan Kaufmann, San Francisco, 2000).
- 5) J. A. Moriarty, *Phys. Rev. B* **42** (1990) 1609; *Phys. Rev. B* **49** (1994) 12431.
- 6) S. Rao, C. Hernandez, J. P. Simmons, T. A. Parthasarathy, and C. Woodward, *Phil. Mag. A* **77** (1998) 231.
- 7) A. N. Stroh, *Phil. Mag.* **3** (1958) 625; *J. Math. Phys.* **41** (1962) 77.
- 8) P.H. Dederichs and G. Leibfried, *Phys. Rev.* **188** (1969) 1175.
- 9) H. Schultz and P. Ehrhart, *Atomic Defects in Metals, New Series, Group III* (Springer, Berlin, 1991).
- 10) W. Xu and J.A. Moriarty, *Phys. Rev. B* **54** (1996) 6941.
- 11) V. Vitek, *Cryst. Lattice Defects* **5** (1974) 1.
- 12) M.S. Duesbery and V. Vitek, *Acta Mater.* **46** (1998) 1481; S. Ismail-Beigi and T.A. Arias, *Phys. Rev. Lett.* **84** (2000) 1499; C. Woodward and S.I. Rao, *Phil. Mag. A* **81** (2001) 1305.
- 13) J.P. Hirth and J. Lothe, *Theory of Dislocations* (Wiley-Interscience, New York, 1982).